The influence of weather and weather variability on mosquito abundance and infection with West Nile virus in Harris County, Texas, USA

Karen C. Poh [a], Luis F. Chaves [b], Martin Reyna-Nava [c], Christy M. Roberts [c], Chris Fredregill [c], Rudy Bueno Jr. [a], Mustapha Debboun [c], Gabriel L. Hamer [a],*

[a] Department of Entomology, Texas A&M University, College Station, TX, USA
[b] Instituto Costarricense de Investigación y Enseñanza en Nutrición y Salud (INCIENSA), Tres Ríos, Cartago, Costa Rica
[c] Mosquito and Vector Control Division, Harris County Public Health, Houston, TX, USA

HIGHLIGHTS

- 10,533,033 female *Culex quinquefasciatus* mosquitoes collected from 2002 to 2015 in Harris County, Texas, USA.
- Time series analysis correlates weather, vegetation, mosquito abundance and infection with West Nile virus.
- Models suggest increased variability in temperature and rainfall increase mosquito abundance, supporting Schmalhausen's law.
- Warmer winter temperatures were related to increased mosquito infection with West Nile virus eight months later.

GRAPHICAL ABSTRACT
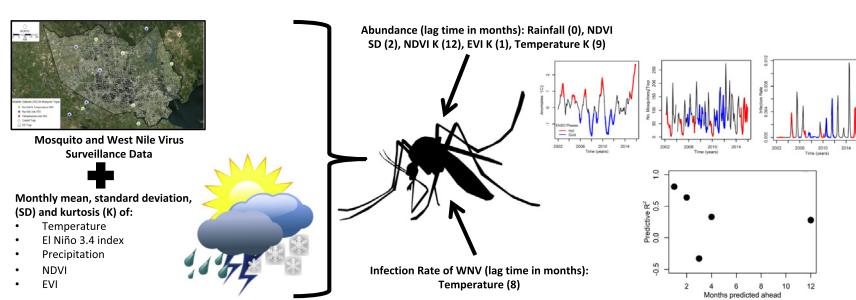
ARTICLE INFO

ABSTRACT

Early warning systems for vector-borne diseases (VBDs) prediction are an ecological application where data from the interface of several environmental components can be used to predict future VBD transmission. In general, models for early warning systems only consider average environmental conditions ignoring variation in weather variables, despite the prediction from Schmalhausen's law about the importance of environmental variability for biological systems. We present results from a long-term mosquito surveillance program from Harris County, Texas, USA, where we use time series analysis techniques to study the abundance and West Nile virus (WNV) infection patterns in the local primary vector, *Culex quinquefasciatus* Say. We found that, as predicted by Schmalhausen's law, mosquito abundance was associated with the standard deviation and kurtosis of environmental variables. By contrast, WNV infection rates were associated with 8-month lagged temperature, suggesting environmental conditions during overwintering might be key for WNV amplification during summer outbreaks. Finally, model validation showed that seasonal autoregressive models successfully predicted mosquito WNV infection rates up to 2 months ahead, but did rather poorly at predicting mosquito abundance, a result that might reflect impacts of vector control for mosquito population reduction, geographic scale, and other artifacts generated by operational constraints of mosquito surveillance systems.

1. Introduction

Early warning systems of vector-borne diseases (VBDs) are crucial to the effective and efficient control of a disease prior to the appearance of

* Corresponding author.
E-mail address: ghamer@tamu.edu (G.L. Hamer).

human infections. To develop early warning systems, a complete understanding of the ecology of the disease system and its extrinsic environmental drivers is necessary. Early warning systems have used a variety of methods and data sources such as vegetation and weather in combination with geographic information systems/remote sensing to predict various VBDs including malaria in Africa, American Cutaneous Leishmaniasis in Costa Rica, dengue in Brazil, and West Nile virus (WNV) in the United States of America (USA), among many other VBDs (Chaves and Pascual, 2007; Connor et al., 1999; Craig et al., 1999; Kuhn et al., 2005; Lowe et al., 2013; Manore et al., 2014; Rogers and Randolph, 2003; Ruiz et al., 2010; Shaman and Day, 2005; Shand et al., 2016; Thomson and Connor, 2000; Thomson et al., 2006).

Most models used in the development of early warning systems for disease prediction have used mean (average) environmental variables as inputs for model development. However, studies suggest that models could be improved by including measurements of environmental variability. For example, it has been observed that higher order statistical moments of environmental variability in weather, such as kurtosis or standard deviation, allow more accurate prediction of abundance in several mosquito species (Chaves, 2016; Chaves et al., 2011a; Chaves et al., 2012; Hayes and Downs, 1980; Ng et al., 2018; Shaman and Day, 2007). This prediction follows Schmalhausen's law, the ecological principle stating that organisms are sensitive to not only average patterns, but also to variability patterns (Chaves and Koenraadt, 2010; Lewontin and Levins, 2000). For instance, organisms are susceptible to variability in their environment when stressed by any single environmental component (Chaves and Koenraadt, 2010; Lewontin and Levins, 2000). In principle, environmental variability can be measured by higher order statistical moments, such as the variance, which measures a variable's dispersion around its mean (Fig. S1A). Another example is kurtosis, which measures whether a variable is more unpredictable on the extremes of a distribution with respect to the mean, generating a leptokurtic distribution, or if an environmental variable is more unpredictable around the mean, generating a platykurtic distribution (Fig. S1B) (Chaves et al., 2011a).

In general, it is expected that biological systems are more sensitive to platykurtic environmental components, provided that there is more uncertainty regarding values around a mean, than in a leptokurtic environment, where there is relatively low variability when the environment fluctuates around the mean (Levins, 1968). Due to their complex biology, VBDs are excellent model systems to test the hypothesis around Schmalhausen's law, given the confluence of many different organisms that have different degrees of autonomy and interactions with changing environments in both their life cycles and the ecological interactions leading to pathogen transmission (Chaves, 2017).

The VBD patterns of interaction with the changing environment might be one of the key components to explain the emergence of new diseases and their successful establishment in new habitats (Levins et al., 1994). Among VBDs, WNV is a zoonotic disease with an enzootic cycle involving avian amplification hosts and mosquito vectors that recently invaded North America (Weaver and Reisen, 2010). Despite the abundance of studies examining its association with environmental variables (Brown et al., 2008b; Chase and Knight, 2003; Degroote et al., 2014; Randolph and Rogers, 2010; Reisen, 1995; Reisen et al., 2008; Reisen et al., 2006a; Reisen et al., 2006b; Reisen et al., 2010; Ruiz et al., 2010; Shand et al., 2016), little to no studies inquire about the impacts of environmental variability on its transmission.

West Nile virus is a pathogen that was first introduced to the USA in 1999, and has since spread throughout North America. Since its introduction in the USA, 46,086 cases of WNV and 2,017 deaths have been recorded as of 2016 (CDC, 2016). The WNV transmission cycle involves avian hosts that amplify the virus acquired via infected mosquito bites, and then can infect bloodsucking mosquitoes that continue transmission among avian hosts or bridge transmission to "dead-end hosts," such as horses and humans, which are not able to infect mosquitoes

(Weaver and Reisen, 2010). *Culex* spp. mosquitoes are the primary WNV enzootic and amplification vectors (Turell et al., 2005; Weaver and Reisen, 2010), and also one of several species capable of "bridge transmission" between animal and human hosts (Hamer et al., 2008a; Hamer et al., 2008b; Kilpatrick et al., 2005).

The amplification of WNV is highly heterogeneous each season, with periodic outbreak years mixed with low levels of virus transmission, and weather is one of the suggested key factors driving these patterns (Chung et al., 2013; Ruiz et al., 2010). For example, weather plays a vital role in the abundance of mosquito populations and subsequent pathogen transmission (Chaves, 2017). Increasing ambient temperature, up to a point, will increase the rate of development, productivity, and abundance of mosquito populations and decrease the extrinsic incubation period, which is the time interval between the uptake of an infectious blood meal until the mosquito is capable of transmitting the virus (Dohm et al., 2002; Reisen et al., 2006b; Rueda et al., 1990; Smith, 1987).

In addition, precipitation is known to have important consequences on mosquito productivity and abundance (Chuang et al., 2011; Degroote et al., 2014; Ruiz et al., 2010), which also influences WNV transmission. However, the influence of prior precipitation on WNV transmission is complex and no clear patterns have emerged from multiple studies (Chuang et al., 2012; Chung et al., 2013; Landesman et al., 2007; Paz and Semenza, 2013). Precipitation creates small pools of water that become enriched, creating suitable oviposition habitats for gravid female mosquitoes (Britton, 1914; Calhoun et al., 2007; Soverow et al., 2009; Takeda et al., 2003). *Culex quinquefasciatus* Say can often be found in artificial containers that are common in urban environments (Andreadis, 2012; Diaz-Badillo et al., 2011; Vezzani, 2007) and this mosquito species selects nutrient enriched habitats (Chaves et al., 2009). The survival of *Cx. quinquefasciatus* mosquitoes relies on these containers because they are often filled with enriched organic material and water collected from precipitation (Chaves et al., 2011b; Ponnusamy et al., 2008). However, heavy rainfall can flush larval habitats and reduce adult mosquito productivity (Koenraadt and Harrington, 2008; Shaman et al., 2002). Furthermore, drought conditions can disrupt the aquatic ecosystem of predators and competitors that serve to limit mosquito larval activity, allowing larvae to fully develop and emerge as adults (Chase and Knight, 2003).

Temperature and precipitation can affect the amount of vegetation present. Vegetation can serve as resting habitats for adult mosquitoes, roosting sites for avian hosts that female mosquitoes utilize for a blood meal, and sources of nutrition during the development cycle of the immature stages of mosquitoes (Brown et al., 2008a; Gardner et al., 2013; Ward et al., 2005).

Texas has experienced consistent epidemics contributing 12.0% and 14.0% of the national human WNV cases and deaths, respectively (CDC, 2016). During the largest epidemic of WNV in 2012, Texas contributed 1868 total cases (West Nile fever and West Nile neuroinvasive disease) and 89 deaths, which was 32.9% of the cases and 31.1% of the deaths reported that year, respectively (CDC, 2016). The costs associated with this outbreak including medical care, vector control, and productivity loss were estimated to be approximately $47.6 million (Murray et al., 2013). Given the significant economic loss associated with WNV, it is important to understand the ecology of WNV transmission dynamics as a key role for effective intervention strategies. Quantitative predictive models as part of an early warning system for WNV transmission have been developed for certain regions of the USA, but they have not been parameterized for Texas, USA. In central and southeast Texas, the southern house mosquito *Culex quinquefasciatus* is the most relevant mosquito species involved in the transmission cycle (Lillibridge et al., 2004; Molaei et al., 2007). Being able to predict when and where WNV infection in the *Culex* mosquito population is greatest provides an early warning system and the opportunity to control mosquitoes before bridge transmission to humans and alert the public with the appropriate messages to reduce WNV exposure risk.

Utilizing a long-term dataset from Harris County, Texas, USA we examined the influence of weather patterns, including mean conditions and higher order statistical moments like standard deviation (SD) and kurtosis, on the abundance and WNV infection of *Cx. quinquefasciatus*, the main WNV vector in southeast Texas. We hypothesized that annual and seasonal weather patterns affect mosquito biology and WNV transmission dynamics, which contribute to the temporal heterogeneity in the abundance and WNV infection rates of *Cx. quinquefasciatus*. We also expected that previous winter temperatures, which set the conditions for mosquito overwintering (Chaves et al., 2018; Chung et al., 2013; Dohm and Turell, 2001; Reisen et al., 2006a), might influence *Cx. quinquefasciatus* WNV infection rates in the subsequent summer, thus creating the expectation of long delays in the association between temperature and WNV infection rates in *Cx. quinquefasciatus*.

2. Materials and methods

2.1. Study area

Harris County, TX includes the metropolitan city of Houston and has a population of 4.7 million people according to the 2017 USA Census estimates, making it the most populated county in Texas and the third most populated county in the USA (United States Census Bureau, 2018). Its unique location along the Gulf makes it prone to severe weather such as hurricanes, which result in major flooding events. To counteract flooding events, Harris County has a large flood control system comprised of several different water containment parts, such as bayous, channels, storm drains, and sewers, many of which are aging and rich with organic materials suitable for mosquito breeding (Molaei et al., 2007). Following outbreaks of St. Louis Encephalitis (SLE) virus, a similar arbovirus to WNV, which amplifies in *Culex* mosquitoes and birds with spillover transmission to humans, Harris County first began its mosquito surveillance program in 1965. Since then, the surveillance program has generated considerable mosquito disease research, expanded their surveillance to include WNV, dengue, chikungunya, and Zika viruses, and generated a robust long-term mosquito abundance and WNV infection dataset (Dennett and Debboun, 2017). Other publications have focused on the most populous areas

within the I-610 highway loop, which mainly comprises Houston (Curtis et al., 2014; Dennett et al., 2007a; Rios et al., 2006), however, this study will analyze data from the entire county.

2.2. Mosquito data

Harris County Public Health Mosquito and Vector Control Division (HCPH MVCD) conducted weekly mosquito surveillance from 2002 to 2016. HCPH MVCD consistently used a combination of storm sewer (SS) and gravid (GV) traps for WNV surveillance throughout the county (Fig. 1). The SS traps are modified CDC Light Traps baited with dry ice and attached to man hole covers underground to attract host-seeking mosquitoes (Molaei et al., 2007). The GV traps mainly attract ovipositing adult female mosquitoes and are baited with hay infusion water and placed in residential yards, usually under vegetation. The hay infusion is composed of mixing 1.3 kg of Coastal bermudagrass, *Cynodon dactylon* (L.), with 42 gal of water and then aged for 10–14 days (Dennett et al., 2007b; White et al., 2009). Other trap types used by HCPH MVCD included under-house traps, which are CDC traps baited with dry ice and placed in crawl spaces underneath houses (Morris and DeFoliart, 1969), and BG traps, which are baited with BG lures from Biogents (Regensburg, Germany). While HCPH MVCD used a combination of traps, only data from SS and GV traps were analyzed given their ubiquitous usage throughout the study period and the county.

The mosquito collection protocol from Harris County has been described in detail elsewhere (Curtis et al., 2014; Molaei et al., 2007). Briefly, traps are placed in the afternoon between 1:30 PM and 5:00 PM and then collected the following morning between 7:30 AM and 10:30 AM. Traps are placed into "operational areas," which are comprised of lines that divide the county for surveillance, inspection, and control operations (Hunt and Hacker, 1984). The 268 operational areas are based on municipal, district, and zip code lines. Live mosquitoes were brought back to the laboratory and frozen at −70 °C. Mosquitoes were identified by species and sex by using keys in Darsie Jr. and Ward (2005) and on a chill table to preserve the presence of the virus and then sorted into pools of ≤50 mosquitoes, with a maximum of three pools per trap. Mosquito abundance was estimated as the average
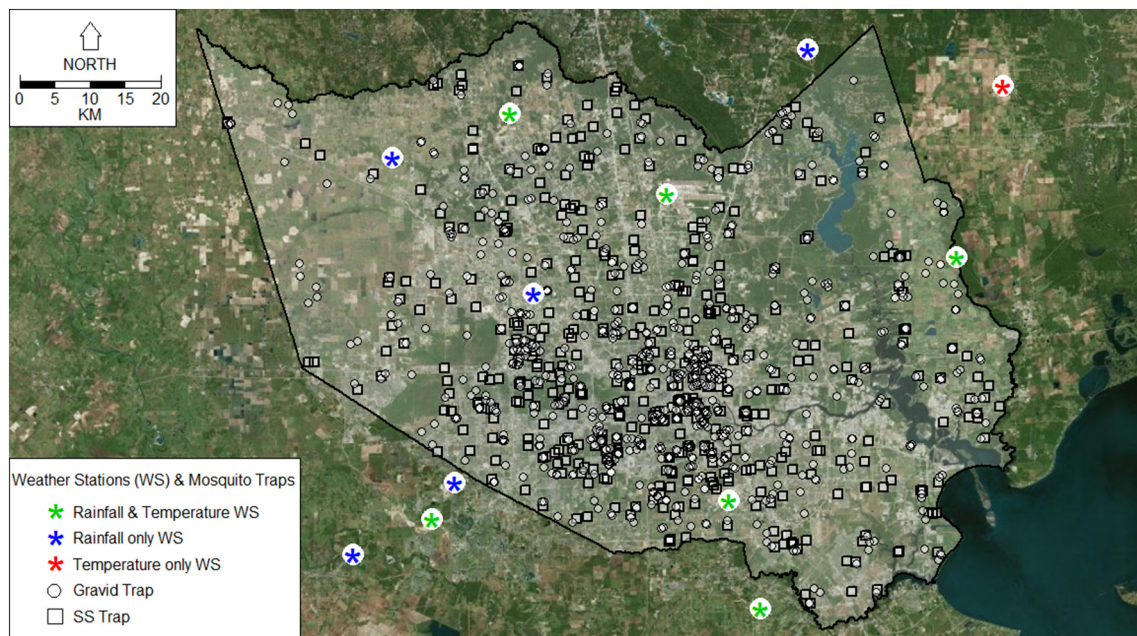

Fig. 1. Map of Harris County, weather stations and trap locations. The background map is courtesy of Google Earth – Harris County is highlighted and the location of mosquito traps, gravid and storm-sewer (SS) traps, are indicated with different symbols. Weather stations are color coded according to whether they recorded temperature and rainfall, only rainfall, or only temperature. For details about symbols and color codes, please refer to the inset legend.

number of mosquitoes trapped during one trap-night. Thus, monthly abundance estimates are the total number of mosquitoes divided by the total number of traps deployed each month. Monthly mosquito abundance was estimated for SS and GV separately, considering these traps collect mosquitoes at different physiological states, and also combined mosquito counts from both traps, assuming this estimate will be more representative of field mosquito populations which include both host-seeking and ovipositing females. The HCPH MVCD Virology Laboratory tested for WNV antigen in mosquito pools using an enzyme-linked immunosorbent assay (ELISA) and positive results were confirmed with a Rapid Analyte Measurement Platform (RAMP) test (Lillibridge et al., 2004; Randle et al., 2016). To be considered a positive pool, the mosquito pool must test positive on both the ELISA and RAMP test. A positive pool is a mosquito pool that contains at least one *Cx. quinquefasciatus* mosquito positive for WNV. Using data from all the pools tested, we estimated monthly infection rates under the assumption that the diagnostic methods have a sensitivity near 1, using a maximum likelihood estimation method for unequal pool size that is fit with a complimentary log-log link generalized linear model (Farrington, 1992) and confidence intervals that are estimated by inverting a likelihood ratio test (Rigg et al., 2019; Speybroeck et al., 2012). None of our monthly estimates were based on a sample where all pools were positive for WNV.

When generating the time series, we inputted missing values for December 2003 and January 2004, when no traps were deployed by HCPH MVCD, which was done via interpolation using a loess regression as described by Ng et al. (2018).

2.3. Weather and vegetation data

For this study, we acquired data for global climatic indices and local weather for Harris County, TX. To evaluate the impact of global climatic phenomena on *Cx. quinquefasciatus* abundance and its WNV infection rate, we downloaded monthly data for the Niño 3.4 index from the USA National Oceanic and Atmospheric Administration (NOAA) Climate Prediction Center (NOAA National Weather Service, 2018). The Niño 3.4 index is associated with interannual rainfall dynamics in Texas (Li and Kafatos, 2000), based on the Extended Reconstructed Sea Surface Temperature version 5 (Huang et al., 2017), and corresponds to sea surface temperatures measured in the area delimited by 5°N–5°S and 170°W–120°W of the Pacific Ocean. Furthermore, the Niño 3.4 index defines the two alternate states during the El Niño Southern Oscillation (ENSO), El Niño ("hot ENSO phase," anomalously warm waters in the eastern tropical Pacific Ocean) and La Niña ("cold ENSO phase," anomalously cool waters).

To evaluate the impact of local climatic indices in our data, we used data from weather stations located inside Harris County or neighboring counties (Fig. 1). We used the Climate Data Explorer from the Royal Netherlands Meteorological Institute (KNMI, 2018) to download daily weather data, and searched for stations that had at least 10 years of data. We specifically selected the following weather stations (coordinates and Global Historical Climatological Network (GHCN) Code) (Fig. 1): Baytown (29.91°N, −94.99°E, USC00410586), Clover Field (29.52°N, −95.24°E, USW00012975), Hobby Airport (29.64°N, −95.28°E, USW00012918), Houston Intercontinental Airport (29.98°N, −95.36°E, USW00012960), Hooks Airport (30.07°N, −95.56°E, USW00053910), and Sugarland (29.62°N, −95.66°E, USW00012977), which had both temperature and rainfall records for our study period. Stations that had data for only rainfall included: Cypress (30.02°N, −95.71°E, USC00412206), New Caney (30.14°N, −95.18°E, USC00416280), North Houston (29.87°N, −95.53°E, USC00414327), Richmond (29.58°N, −95.76°E, USC00417594), and Westbury (29.66°N, −95.63°E, USC00414325). Data for only temperature was available at Dayton (30.10°N, −94.93°E, USR0000TDAY).

We processed the daily data to generate monthly time series for the study period. We computed the monthly mean, SD, and kurtosis for

temperature and rainfall in Harris County. The SD and kurtosis estimates were based on daily temporal and spatial data from the weather stations in Fig. 2. For comparison, we also downloaded from the Earth System Research Laboratory (ESRL) gridded weather data from Global Historical Climatology Network/Climate Anomaly Monitoring System (GHCN/CAMS) 2 m (temperature) (NOAA ESRL, 2018a) and global precipitation climatology project (GPCP) (rainfall) (NOAA ESRL, 2018b), with resolutions of 0.5° and 0.25°, respectively, which were only available as monthly averages based on daily data.

We downloaded monthly images for vegetation indices with a 1-km resolution vegetation (M*D13A3) based on MODIS satellite images (Didan, 2015). The Normalized Difference Vegetation Index (NDVI) and Enhanced Vegetation Index (EVI) are considered proxies for vegetation growth (Pettorelli et al., 2005). The images, which are courtesy of the NASA Land Processes Distributed Active Archive Center (LP DAAC), United States Geological Survey (USGS)/Earth Resources Observation and Science (EROS) Center (Sioux Falls, South Dakota), were downloaded from the server (NASA, 2018) using the package *MODIStsp* for the software R (Busetto and Ranghetti, 2016). Each image was clipped to the surface of Harris County, and stacked into a geotiff using the package *raster* for R (Brunsdon and Comber, 2015). For each monthly image, we estimated the mean, SD and kurtosis for NDVI and EVI during the study period, which were based on information from the image pixels.

2.4. Statistical analysis

2.4.1. Seasonality

Seasonal profiles for all the mosquito time series, vegetation, and weather variables were built using monthly boxplots (Venables and Ripley, 2002).

2.4.2. Non-stationary patterns of association in the time series

We studied the association of cycles in the time series using a cross wavelet coherence analysis to identify non-stationary association patterns (i.e., changes through time) and the association between cycles in the time series, or coherence, whose period might be variable and not repetitive or seasonal (Cazelles et al., 2007; Chaves and Pascual, 2006). We used this technique to study the association between mosquito abundance and infection with the Niño 3.4 index, NDVI, EVI, temperature, and rainfall.

2.4.3. Time series modeling

To fit and select variables for monthly time series models of mosquito abundance and WNV infections in pools, we used a standard protocol for the time series analysis (Hurtado et al., 2014; Hurtado et al., 2018). The first step consists of assessing the correlation of each time series with itself by inspecting the autocorrelation function (ACF) as well as the correlation of consecutive time lags using a partial autocorrelation function (PACF) (Shumway and Stoffer, 2011). Information from the ACF and PACF will identify a null model that considers the autocorrelation structure of the focal time series. This null model was used to pre-whiten the times series with the Kalman filter. Pre-whitening is a process to remove a common autocorrelative structure that can generate spurious correlations from the climate, weather, and vegetation indices (Shumway and Stoffer, 2011). Residuals from the autonomous model and the pre-whitened time series were used to estimate cross correlation functions (CCFs), which show the correlation between two time series as a function of fixed time lags (Hoshi et al., 2014). Once we identified significant lags of the covariates between 1 and 12 months ($P < 0.05$), the lags were used to fit full models of mosquito abundance and mosquito WNV infection. Models were simplified by model selection through backward elimination (Kuhn and Johnson, 2013), following the minimization of the Akaike Information Criterion (AIC) (Faraway, 2016). This process allows model selection among models with similar parameter numbers (Faraway, 2016). For the
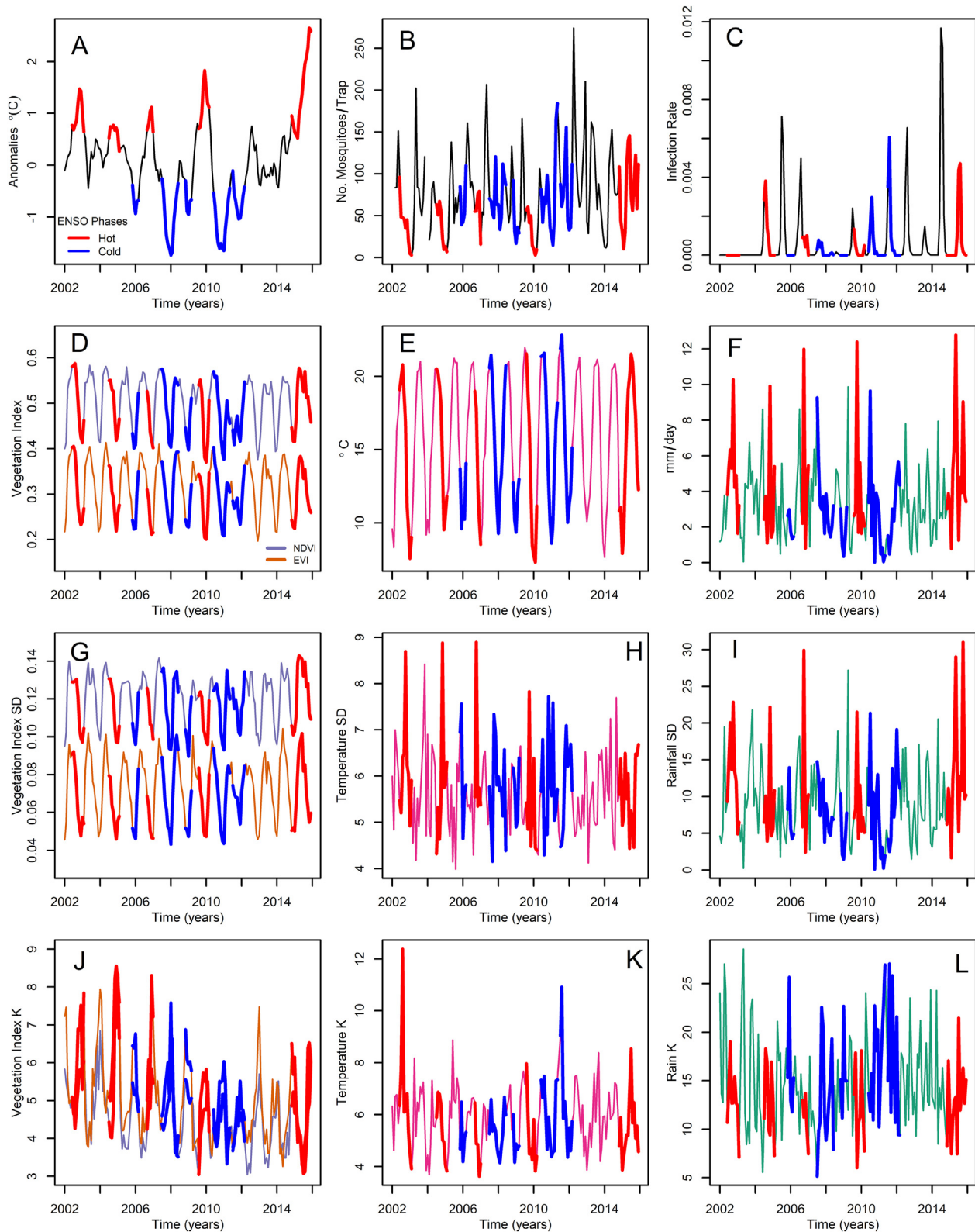
Fig. 2. Monthly time series. (A) Sea surface temperature in the El Niño 3.4 region (Niño 3.4) (°C) (B) average number of mosquito per trap (C) West Nile virus mosquito infection rate (D) vegetation indices, including the Normalized Difference Vegetation Index (NDVI), and the Enhanced Vegetation Index (EVI) (E) average temperature (°C) (F) average rainfall (mm/day) (G) standard deviation, SD, of NDVI and EVI (H) SD of temperature (I) SD of rainfall (J) kurtosis, K, of NDVI and EVI (K) K of temperature (L) K of rainfall. In all panels ENSO phases are highlighted by colors, for details, see inset legend of panel A. Panels B and C are based on combined data from gravid and storm sewer traps. In panels D, G and J NDVI and EVI are differentiated by color, see inset legend of panel D for details.

best-fit models, we tested if variables, whose parameters were not significant, could be eliminated using likelihood ratio tests (Faraway, 2016), and the resulting models are reported as the best models in the

Results section. For the best models, we verified time series model assumptions using standard procedures for the time series analysis (Shumway and Stoffer, 2011).

2.4.4. Time series model validation

We validated the time series models by leaving observations from 2016 out of the model fitting and forecasted mosquito abundance and WNV infection rates at time steps of 1, 2, 3, 4, 6 and 12 months. We tested the predictive ability of the model by estimating the predictive R^2 (Chaves and Pascual, 2007), which is defined as the variance normalized mean square error of the prediction, i.e.

$$_{Pred}R^2 = 1 - (\text{mean square error}/\text{variance of the series}). \tag{1}$$

The predictive R^2 has a straightforward interpretation, where a $_{Pred}R^2$ of 1 indicates perfect forecasts, but a negative value, or near 0, indicates a poor predictive ability (Chaves and Pascual, 2007).

3. Results

Data time series are shown in Fig. 2, where color codes are used to represent the phases of ENSO. During the study period, the most extreme ENSO occurred in 2015–2016, as shown by the Niño 3.4 index time series (Fig. 2A).

The HCPH MVCD used 686 and 476 locations for GV and SS traps throughout Harris County, respectively. A total of 10,533,033 female *Cx. quinquefasciatus* were collected using GV (5,371,840 mosquitoes, 51% of the samples) and SS (5,161,193 mosquitoes, 49%) traps. The total sampling effort, which is defined as the amount of mosquito trapping deployed for surveillance by Harris County, was 130,567 trap-nights, with 55% of the sampling effort from GV traps (71,849 trap-nights) and the remaining 45% from SS traps (58,718 trap nights). Monthly mosquito abundance, based on combined GV and SS trap collections, was highly variable (Fig. 2B), having an average ($\pm$SD) of 74.84 $\pm$ 47.89. Meanwhile, the average abundance for GV and SS traps was 67.49 $\pm$ 41.94 and 79.85 $\pm$ 64.05, respectively. Mosquito abundance peaks were observed when ENSO was not going through its hot and cold phases, a pattern also observed for the time series based on GV (Fig. S2A) and SS (Fig. S2B) traps.

The monthly average WNV infection rate ($\pm$SD), estimated only for months with positive pools, was 0.00158 $\pm$ 0.00235, which is a proportion, i.e., for each 10,000 tested mosquitoes, around 16 were infected by WNV. As observed with mosquito abundance, WNV infection peaks were observed at times when ENSO activity did not go through the hot and cold phases, but overall, followed cold ENSO phases (Fig. 2C). Unlike what was observed for mosquito abundance, temporal patterns of mosquito infection were nearly identical when comparing infection estimates from GV (Fig. S2C) and SS (Fig. S2D) traps. For this reason, we used the WNV infection time series based on GV and SS traps for subsequent analyses. The NDVI and EVI had similar temporal patterns during the study period (Fig. 2D), with data suggesting that vegetation growth at Harris County slows down during the cold ENSO phase. Meanwhile, temperature (Fig. 2E) is higher during the cold ENSO phase, and the estimate using station data was very similar to the data from the gridded database (Fig. S2E). Rainfall peaked during the hot ENSO phase followed by the cold phase (Fig. 2F), but this temporal pattern was not clear for the gridded rainfall (Fig. S2F). Given the more apparent patterns of ENSO impacts on the weather observed from weather stations, we used this data for subsequent analyses.

The SDs of the vegetation indices (Fig. 2G) were similar to the mean time series of the vegetation indices. By contrast, the SD of temperature (Fig. 2H) and rainfall (Fig. 2I) reached maximum values during the hot ENSO phase, followed by the cold phase. The vegetation indices (Fig. 2J) and temperature (Fig. 2K) were more leptokurtic during the hot and cold ENSO phases, meaning that most of the variability occurred around the mean value than in the ENSO phases, and more platykurtic when ENSO was not passing through a hot or cold phase. In contrast, rainfall (Fig. 2L) was most leptokurtic during the cold ENSO phase and most platykurtic during the hot ENSO phase.

Seasonal patterns of mosquito abundance for *Cx. quinquefasciatus*, based on both GV and SS traps, (Fig. 3A) were bimodal having a large peak in May and a second small peak in November. When separating the abundance by trap type, this bimodal pattern was not observed in GV traps, which had a single peak in May (Fig. S3A). However, the bimodal seasonality was observed in SS traps (Fig. S3B), which had peaks in May and November. Given these marked differences in abundance between GV and SS traps, we decided to perform time series analyses of the combined abundance time series, but also of mosquito abundance based on GV and SS traps separately.

Seasonal WNV infection patterns were unimodal with a seasonal peak in August (Fig. 3B), a pattern also observed separately for GV (Fig. S3C) and SS (Fig. S3D) traps. The NDVI has a seasonal peak from April to August (Fig. 3C), while EVI (Fig. 3D) has a unique peak in May. Temperature also had a unimodal pattern (Fig. 3E), with a peak in August, which was also observed in the gridded temperature data (Fig. S3E). Rainfall had two seasons, one relatively dry from January to April, and a wet season for the rest of the year, with August being consistently the driest month during the wet season (Fig. 3F), a similar pattern was also observed in the gridded data (Fig. S3F).

The cross wavelet coherence analyses show that interannual cycles, with a period between 3 and 4 years, of mosquito abundance (Fig. 4A) and WNV mosquito infection rates (Fig. 4B) were coherent with those observed in ENSO. Briefly, this is inferred by looking at the y-axis of the plot through time, i.e., the x-axis. In the y-axis, scale indicates the period of the cycles, and the coherence, which is coded by colors, measures the overlap in cycles present in the studied time series. Coherence varies between 0 and 1 and can be interpreted like a correlation estimate, where values near 1 indicate a near perfect association in the cycles of the studied time series and values close to 0 represent an independence of cycles at a given time scale (Chaves et al., 2014). Meanwhile, NDVI and EVI had seasonal cycles, with periods of 1 year, associated with mosquito abundance (Fig. 4C, E) and WNV infection rate (Fig. 4D, F). Temperature cycles were both seasonal and interannual, with cycles of 2 to 4 years, coherent with mosquito abundance (Fig. 4G) and WNV infection rates (Fig. 4H). Meanwhile, rainfall cycles were associated at an interannual scale, with cycles of 3 to 4 years, with cycles of mosquito abundance, which between 2002 and 2010 were also highly coherent at the seasonal scale with rainfall, (Fig. 4I) and with WNV infection rates (Fig. 4J).

The autocorrelation functions of mosquito abundance (Fig. 5A) and WNV infection rates (Fig. 5B) suggested that both time series were at most second order (autocorrelated up to the second lag) and seasonal (significantly correlated at lag 12 months), meaning time series were seasonally autocorrelated with a 12-month lag. That autocorrelation structure was observed using the partial autocorrelation function of both mosquito abundance (Fig. 5C) and WNV infection rates (Fig. 5D).

With this information, a seasonal autoregressive model was fitted as the null model with the following form:

$$x_t = \mu + \varphi_1 x_{t-1} + \varphi_2 x_{t-2} + \varphi_{12} x_{t-12} - \varphi_1 \varphi_{12} x_{t-13} - \varphi_2 \varphi_{12} x_{t-14} + \varepsilon_t \tag{2}$$

where μ is the mean of the time series $x_t = y_t - \mu$, where y_t is either monthly mosquito abundance or WNV infection rates, t indicates time, and ε_t is a normally and identically distributed error. Model selection for mosquito abundance, the model presented in Eq. (2), suggested that the following model:

$$x_t = \mu + \varphi_1 x_{t-1} + \varphi_{12} x_{t-12} - \varphi_1 \varphi_{12} x_{t-13} + \varepsilon_t \tag{3}$$

was the best null model for abundance estimates based on the combined SS and GV data. This null model was used to pre-whiten the time series of the weather and vegetation covariates, which were then used to estimate cross-correlation functions between the average values of the covariates with mosquito abundance (Fig. 5E) and WNV infection rate (Fig. 5F), the SD of the covariates with mosquito
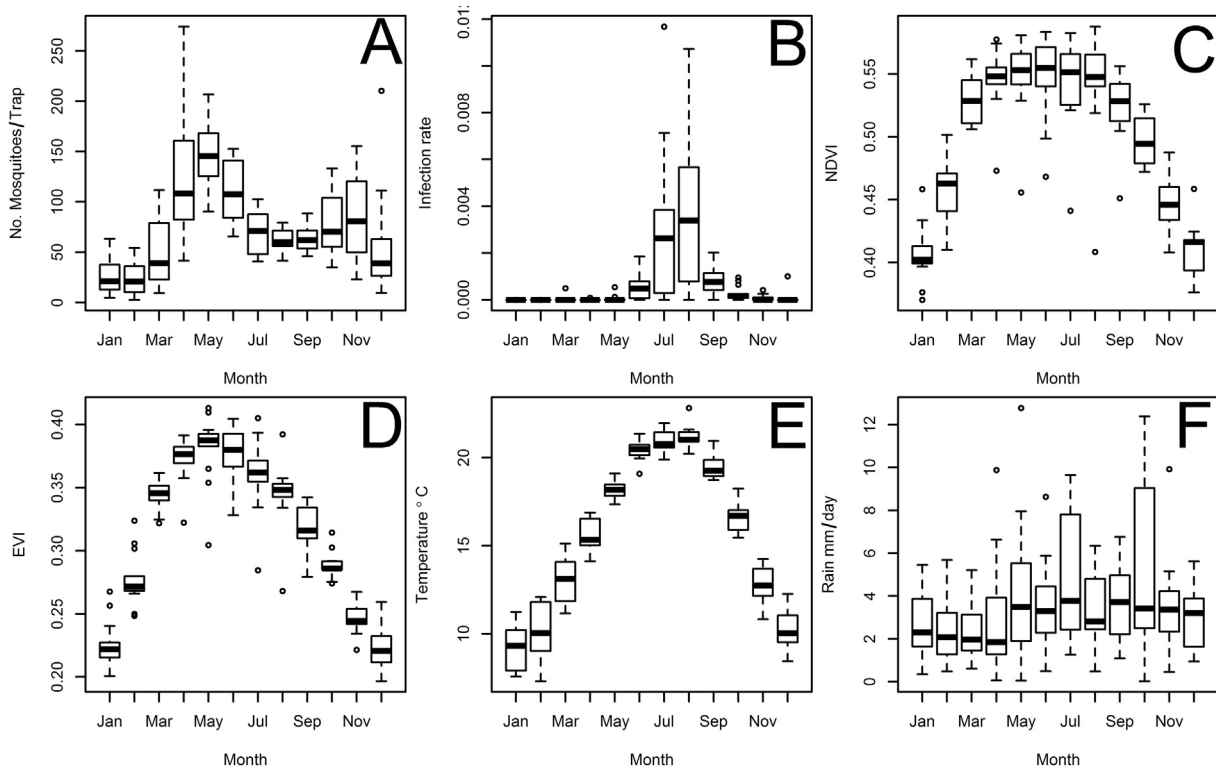
Fig. 3. Seasonal monthly boxplots. (A) Average number of mosquito per trap (B) West Nile virus mosquito infection rate (C) Normalized Difference Vegetation Index (NDVI) (D) Enhanced Vegetation Index (EVI) (E) average temperature (°C) (F) average rainfall (mm/day). Panels A and B are based on combined data from gravid and storm sewer traps.

abundance (Fig. 5G) and WNV infection rate (Fig. 5H), and the kurtosis of the covariates with mosquito abundance (Fig. 5I) and WNV infection rate (Fig. 5J). We also estimated the ACF and PACF of mosquito abundance with GV (Fig. S4A, C) and SS traps (Fig. S4B, D), and the cross-correlation function of mean, SD, and kurtosis of the covariates with GV (Fig. S4E, G, I) and SS (Fig. S4F, H, J) traps.

The variables that were significantly associated with mosquito abundance were then considered in a full model:

$$x_t = \mu + \varphi_1 x_{t-1} + \varphi_{12} x_{t-12} - \varphi_1 \varphi_{12} x_{t-13} + \sum cov_{t-j} + \varepsilon_t \qquad (4)$$

that included covariates (*cov*) with time lags $j \geq 0$. The process of model selection for the mosquito abundance model based on GV and SS traps, the abundance model based only on GV traps, and the abundance model based only on SS traps is presented in Tables S1, S2, and S3, respectively.

Parameter estimates for the best mosquito abundance model are presented in Table 1. Parameters included a positive association with the standard deviation of NDVI (2-month lag) and temperature kurtosis (9-month lag). Meanwhile, abundance was negatively associated with rainfall (no time lag), NDVI kurtosis (12-month lag) and EVI kurtosis (1-month lag). Significant parameters in the best models for mosquito abundance based on GV and SS traps separately (Table S4) had similarities with the model based on data from both traps (Table 1). Both of those models did not have a significant seasonal autoregressive parameter, i.e., both time series were not significantly autocorrelated with themselves with a 12-month lag. Interestingly, both of these models (Table S4) were associated with EVI kurtosis with 1 month of lag, the association being negative like in the model of Table 1. Other parameters shared with the model presented in Table 1 also had the same sign such as the kurtosis of NDVI with a 12-month lag and a 9-month lag temperature kurtosis for the model based on SS traps (Table S4). Other parameters included variables that were not included in the best model presented in Table 1, and included both mean, SD, and kurtosis parameters (Table S4).

The best model for mosquito WNV infection rates (Table 2) was a second order seasonal autoregressive model, i.e., with an autoregressive component similar to the one described in Eq. (2), with mean temperature at an 8-month lag as a significant covariate. The process of model selection is shown in Table S5, which showed that WNV infection rate was not significantly associated ($P > 0.05$) with mosquito abundance.

Finally, the process of model validation suggested the predictive ability of the mosquito abundance model was overall low (Fig. 6A), a pattern shared with the models based on GV (Fig. S5A) and SS (Fig. S5B) traps separately, which nevertheless outperformed the model combining the data from both types of traps. By contrast, the predictive accuracy of the WNV infection rate (Fig. 6B) model was high for 1 (80%) and 2 (60%) months, negative at 3 months, and overall decreased as the prediction step increased the number of months predicted at once.

4. Discussion

Our study found significant weather factors and measurements of their variability significantly associated with *Cx. quinquefasciatus* abundance and WNV infection rates during the study period (2002–2016) in Harris County, TX. Mosquito abundance generally peaked following the cold phases when ENSO activity did not go through distinct hot or cold phases (Fig. 2B). During the hot ENSO phase, we generally saw peaks in rainfall and greater variation in temperature and rainfall (Fig. 2). On the other hand, the cold ENSO phases were characterized by hotter temperature peaks and less rainfall, which resulted in less vegetation growth in Harris County (Fig. 2). During these hot and cold ENSO phases, we found lower *Cx. quinquefasciatus* abundance, which could be due to the excess rainfall and higher temperatures/low vegetation in the hot and cold phases, respectively. The increased amount of precipitation during the hot ENSO phase might wash out larval habitats for *Cx. quinquefasciatus* above- and belowground (Koenraadt and Harrington, 2008; Shaman et al., 2002). This phenomenon was true for *Cx.*
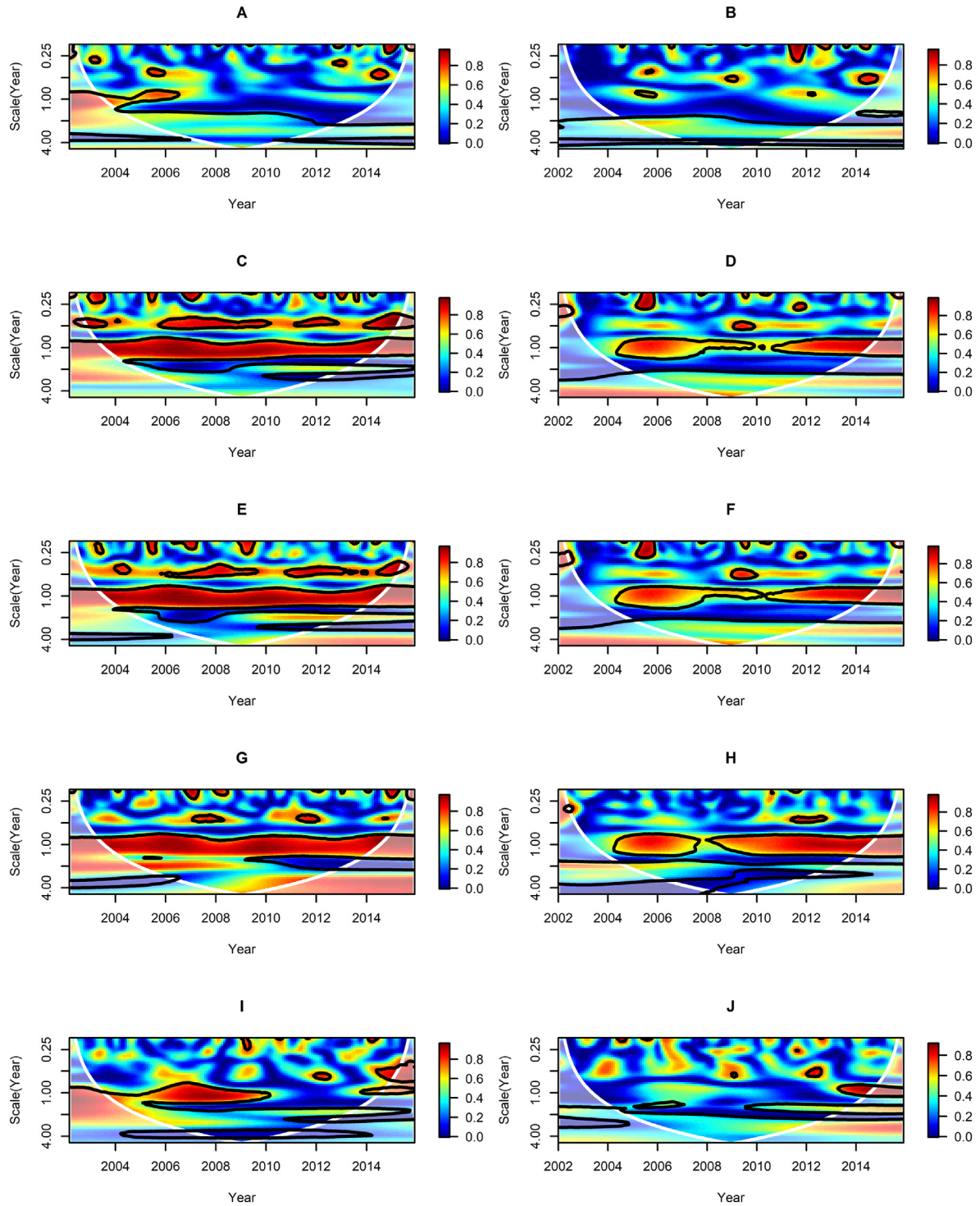
Fig. 4. Cross wavelet coherence analysis. Coherence between sea surface temperature 3.4 (Niño 3.4) and (A) monthly average mosquito abundance per trap (MAMAPT) (B) West Nile virus mosquito infection rate (WNVMIR). Normalized Difference Vegetation Index (NDVI) and (C) MAMAPT (D) WNVMIR. Enhanced Vegetation Index (EVI) and (E) MAMAPT (F) WNVMIR. Temperature and (G) MAMAPT (H) WNVMIR. Rainfall and (I) MAMAPT and (J) WNVMIR. In all plots the y-axis presents the scale, or period measured in years, at which two time series are coherent, while the x-axis represents time. A guide for coherence values is presented to the right of each panel. Coherence goes from zero (blue) to one (red). Red regions in the plots indicate frequencies and times for which the two series share power (i.e., variability). The cone of influence (where results are not influenced by the edges of the data) and significantly coherent (P < 0.05) scales through time are indicated by solid lines. MAMAPT and WNVMIR are based on combined data from gravid and storm sewer traps.

quinquefasciatus in the USA as observed in California (Heft and Walton, 2008) and Georgia (Chaves and Kitron, 2011; Nguyen et al., 2012) and *Cx. pipiens* in Illinois (Hamer et al., 2011). Extremely high temperatures are known to decrease the life span of the mosquito and prematurely kill mosquitoes before they are able to transmit the virus to a new host (Brault, 2009; Reisen, 1995; Reisen et al., 2006b). Vegetation is

required for larval development of *Cx. quinquefasciatus* as it provides a source of organic matter and nutrients. The importance of vegetation has been investigated in other areas of the USA such as the cities of New York, Chicago and Houston, where the presence of vegetation was positively associated with human risk for WNV (Brownstein et al., 2002; Nolan et al., 2012; Ruiz et al., 2004).
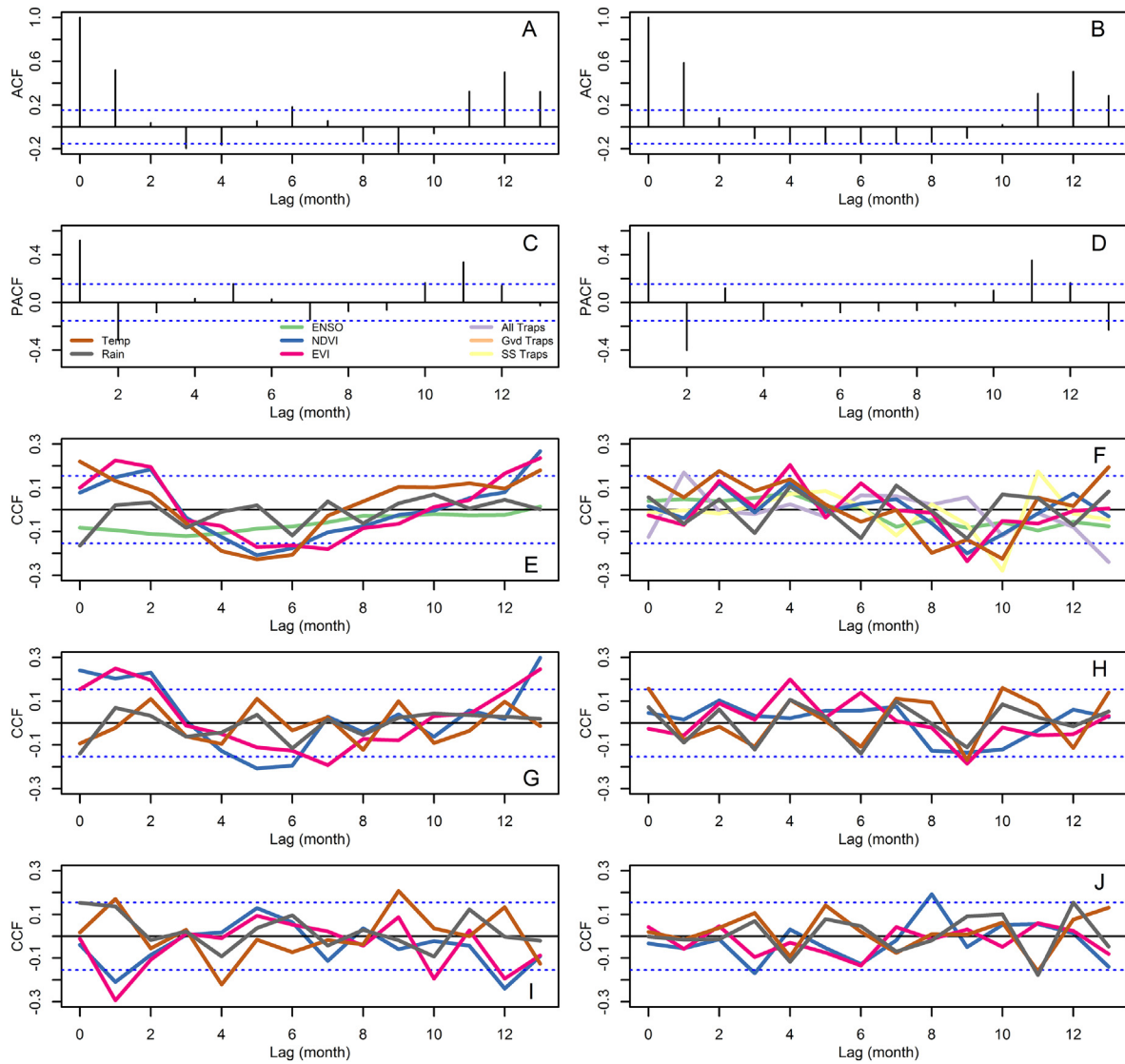
Fig. 5. Correlation functions. Auto-Correlation function, ACF of (A) monthly average mosquito abundance per trap (MAMAPT) and (B) West Nile virus mosquito infection rate, (WNVMIR). Partial Auto-Correlation function, PACF of (C) MAMAPT and (D) WNVMIR. Cross-Correlation functions, CCF of the average value of environmental variables with (E) MAMAPT and (F) WNVMIR. CCF of the standard deviation, SD, of environmental variables with (G) MAMAPT and (H) WNVMIR. CCF of the kurtosis, K, of environmental variables with (I) MAMAPT and (J) WNVMIR. In panels E to J environmental variables are color coded, for details, please refer to the insect legend of panel D. MAMAPT and WNVMIR are based on combined data from gravid and storm sewer traps.

Our results demonstrate that increased variability in both temperature and rainfall result in higher abundance of mosquitoes. Measurements of variability were significant covariates in the abundance models (Table 1). The significant covariates in the abundance model further highlight the importance in including measurements of environmental variability to investigate association patterns between mosquito
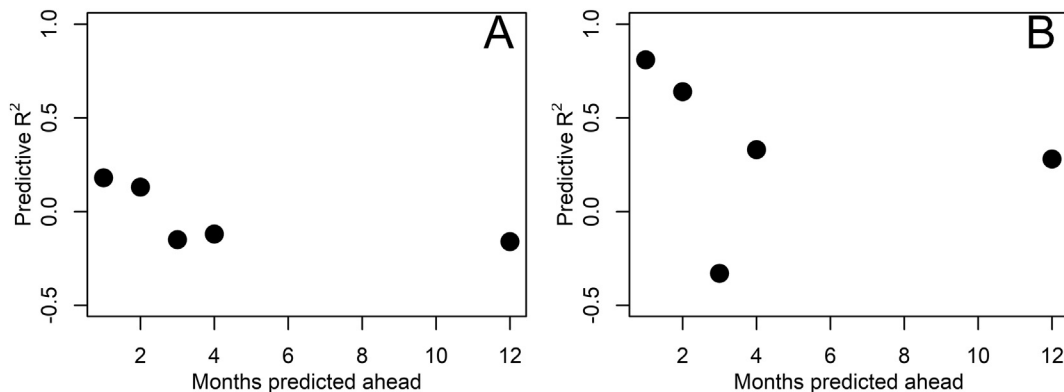

Fig. 6. Predictive R^2 for models selected as best to explain (A) monthly average mosquito abundance per trap (B) West Nile virus mosquito infection rate.

Table 1
Parameter estimates for the best time series model explaining changes in *Culex quinquefasciatus* abundance sampled with gravid and storm-sewer traps in Harris County, TX. $\sigma^2 = 1045$, Log Likelihood $= -705.7$, AIC $= 1429.4$.

Parameters (lag)	Mosquito abundance (GV and SS)	
	Estimates	S.E.
Intercept	74.1795	6.3822
AR (1)	0.3873	0.0790
SAR (12)	0.3414	0.0822
Rainfall (0)	−2.6398	1.0384
NDVI SD (2)	792.7775	379.7516
NDVI K (12)	−14.7881	4.8280
EVI K (1)	−8.8210	3.7416
Temperature K (9)	7.8873	2.4330

abundance dynamics and the weather. The covariates for the best mosquito abundance model that combined mosquito counts from both GV and SS traps included positive associations with the standard deviation of NDVI with a 2-month lag and the kurtosis of temperature with a 9-month lag. Rainfall with no lag, NDVI kurtosis with a 12-month lag, and EVI kurtosis with a 1-month lag had a negative association with mosquito abundance. The phenomenon emphasizing the importance of significant variation in weather and vegetation on mosquito abundance follows Schmalhausen's Law, the biological principle stating that organisms are sensitive to both average environmental conditions and environmental variability, which has been previously reported for *Cx. quinquefasciatus* and other disease vectors (Chaves and Koenraadt, 2010; Hayes, 1975; Hayes and Downs, 1980; Hayes and Hsi, 1975; Ng et al., 2018). Therefore, the more neutral conditions seen when ENSO is not going through distinct hot and cold phases may allow for greater abundance of *Cx. quinquefasciatus*.

Interestingly, our study did not include temperature within the same summer season as a significant variable in either of the abundance or infection rate models, which other studies have found among other mosquito species (Chuang et al., 2011; Degaetano, 2005; Ruiz et al., 2010). This could be due to differences in the life history traits for the mosquito species of interest and the regional effects of weather, which may ultimately result in heterogeneous results when comparing relationships between the weather, mosquito abundance, and infection rates (Ciota et al., 2014; Wimberly et al., 2014). Instead, we found that temperature with an 8-month lag was a significantly positive covariate in our WNV infection rate model (Table 2). Given that infection rates generally peak around August in Harris County (Fig. 3B), warmer temperatures during the winter are expected to increase the infection rates the following summer. In general, warmer winter seasons preceding a WNV season has been a significant factor of interest in other studies using various measurements of WNV, including mosquito abundance of different *Culex* species, infection rates/vector indexes, and human cases (Chung et al., 2013; Degroote et al., 2014; Reisen et al., 2010; Wimberly et al., 2014).

One mechanism for increased infection rates in the summer following a mild winter is that warmer temperatures in the winter allow *Cx. quinquefasciatus* to remain active gonotrophically and maintain their populations. Alternatively, *Cx. quinquefasciatus* can survive through the

Table 2
Parameter estimates for the best time series model explaining changes in West Nile virus infection rate of *Culex quinquefasciatus* in Harris County, TX. $\sigma^2 = 1.373e{-}6$, Log Likelihood $= 765.73$, AIC $= -1519.47$.

Parameters (lag)	Infection model	
	Estimates	S.E.
Intercept	0.0008	0.0001
AR (1)	0.7620	0.0787
AR (2)	−0.3199	0.0797
SAR (12)	0.4757	0.0946
Temperature (8)	0.0003	0.0001

winter by entering quiescence when temperatures drop, but can become active once temperatures increase again (Diniz et al., 2017; Eldridge, 1968; Reisen et al., 1986). Quiescence is a period of non-seasonal dormancy characterized by slowed metabolism in response to environmental stimuli (Clements, 1992). Since *Cx. quinquefasciatus* does not enter diapause and is not hormonally-controlled to enter a state of dormancy, physiological activity can be restored once the stimulus that induces quiescence ceases (Denlinger and Armbruster, 2014; Diniz et al., 2017; Lacour et al., 2015; Vinogradova, 2007). The sustained activity in mosquito populations through warmer winter temperatures also permit the maintenance of low levels of WNV in the overwintering adults as well as the potential for enzootic activity and horizontal activity among birds in the winter or spring (Goddard et al., 2003; Hinton et al., 2015; Montecino-Latorre and Barker, 2018; Nelms et al., 2013). For example, when *Cx. pipiens* is inoculated with WNV and held at reduced temperatures (10 °C) for 21–42 days, the virus is not fully disseminated. Once the mosquito is transferred to an incubation temperature of 26 °C, the dissemination rates increased (Dohm and Turell, 2001). While vertical transmission of WNV is possible, it occurs inconsistently and at very low rates (Goddard et al., 2003). Studies on the effects of overwintering in *Cx. quinquefasciatus* and WNV infection in Texas are worth investigating further.

Another mechanism for increased WNV infection rates during a warm winter relates to the opportunistic feeding patterns of *Cx. quinquefasciatus*, which more frequently feed on avian hosts (Molaei et al., 2007). Warmer winter temperatures can signal the arrival of an early spring, allowing birds to initiate recruitment of young earlier (Forchhammer et al., 1998; Walther et al., 2002). Consequently, increased populations of susceptible juvenile birds are known to fuel the amplification of WNV (Hamer et al., 2008b). Mosquito feeding may coincide with warmer temperatures in the winter, allowing mosquitoes to become infected even during periods of expected low activity since birds may still be viremic or become infected from exposure to feces containing WNV (Dawson et al., 2007; Eldridge, 1968; Hinton et al., 2015).

An interesting observation was the difference in mosquito abundance between GV and SS traps. The GV traps exhibited a unimodal abundance distribution, however, SS traps showed a bimodal distribution (Fig. S2). The second abundance peak for *Cx. quinquefasciatus* trapped in SS traps during November could be attributed to its life history. The SS traps are placed underground in storm sewers and baited to capture host-seeking mosquitoes. However, *Cx. quinquefasciatus* will also use storm sewers as hibernacula or shelter during cooler months to overwinter into the next spring season (Strickman and Lang, 1986). With this in mind, the second peak in the abundance in November could be attributed to the mosquito's retreat into underground storm sewers to avoid harsh winter conditions since this species does not enter diapause, but instead undergoes quiescence when retreating to storm drains (Nelms et al., 2013; Nguyen et al., 2012; Reisen, 2012; Reisen et al., 1986; Reisen et al., 2010; Siirin et al., 2004; Strickman, 1983, 1988; Strickman and Lang, 1986). Dissection studies investigating overwintering techniques in California have demonstrated that *Cx. quinquefasciatus* mosquitoes undergo quiescence rather than diapause, which is the overwintering technique for *Cx. pipiens* Linnaeus and *Cx. tarsalis* Coquillet. However, this type of study, to the best of our knowledge, has not been performed in Texas and warrants further consideration to elucidate overwintering patterns for mosquitoes found in storm drains.

The abundance models for this study performed poorly (Fig. 6A), but the infection rate model performed well when predicting between 1 and 2 months ahead (Fig. 6B). The low predictive ability of the abundance model can be attributed to unavoidable logistical constraints that emerge in large-scale vector surveillance systems such as in Harris County, TX. For example, our model did not consider mosquito control efforts by HCPH MVCD that may have affected local mosquito populations. Mosquito control in Harris County consists of aboveground-

based ultra-low volume (ULV) adulticiding in response to a positive mosquito pool. Within the same week of detecting a positive pool, ULV adulticiding will occur in the operational area (Fredregill et al., 2011). During peak seasons, adulticiding may occur more than once a week, which may affect the abundance of mosquitoes trapped by SS and GV traps that target adult mosquitoes.

Another challenge is related to the temporal and spatial scales of our study. Given the long temporal range of our data, we used a monthly scale for the time series analysis. Having a temporal scale of weekly data would better reflect the finer nuances in mosquito abundance dynamics and improve model predictive ability (Chaves et al., 2013; Chuang et al., 2017). Spatial scale is also an important factor when considering infection data since results and conclusions may differ depending on the scale chosen for the study (Winters et al., 2010). We summarized data over a large spatial scale, with Harris County covering over 4600 km^2. At smaller spatial scales, we might better capture local population dynamics, as observed in more finely grained studies on mosquito population dynamics (Chaves et al., 2013; Ng et al., 2018).

A final factor to consider when explaining the low predictive ability of our mosquito abundance models is the movement of trap locations throughout the county during the study period. A total of 686 and 476 trap locations were used for GV and SS traps, respectively (Fig. 1). Throughout the study period, only 15 GV traps and 24 SS traps remained in the same location (Fig. S6). In contrast, 392 GV traps and 324 SS traps were deployed <50 times at the same location, which demonstrates the lack of consistency in trap locations throughout the study period (Fig. S6). Inconsistencies from trapping may lead to artifacts and biases that do not necessarily reflect local population dynamics of the previous trap locations. The location of the trap influences the mosquito abundance estimates, which may help explain the low predictive capability of the abundance models given that many of these traps moved throughout the study period (Brown et al., 2008c).

5. Conclusions

Our study demonstrated the importance of long-term systematic sampling of mosquitoes to build a predictive model as part of an early warning system. This is the first study in Texas, and overall the southwestern USA, to use a long-term dataset to examine weather factors and variability to explain WNV vector abundance and WNV infection rates. We developed and validated models that can accurately predict WNV infection rates in response to weather phenomena. After one of the largest epidemics of WNV in 2012, which was centered in Dallas County, TX, Harris County can integrate these models into a proactive system to initiate interventions and allocate resources for vector control and disease prevention before the appearance of human WNV cases to prevent another devastating epidemic.

Supplementary data to this article can be found online at https://doi.org/10.1016/j.scitotenv.2019.04.109.

CRediT authorship contribution statement

Karen C. Poh: Conceptualization, Investigation, Data curation, Project administration, Supervision, Writing - original draft, Writing - review & editing. **Luis F. Chaves:** Formal analysis, Investigation, Data curation, Methodology, Software, Supervision, Validation, Visualization, Writing - original draft, Writing - review & editing. **Martin Reyna-Nava:** Data curation, Investigation, Writing - review & editing. **Christy M. Roberts:** Data curation, Investigation, Writing - review & editing. **Chris Fredregill:** Data curation, Investigation, Writing - review & editing. **Rudy Bueno:** Jr. Conceptualization, Data curation, Investigation, Resources, Writing - review & editing. **Mustapha Debboun:** Data curation, Investigation, Resources, Writing - review & editing. **Gabriel L. Hamer:** Conceptualization, Funding acquisition, Investigation, Project administration, Resources, Supervision, Writing - review & editing.

References

Andreadis, T.G., 2012. The contribution of *Culex pipiens* complex mosquitoes to transmission and persistence of West Nile virus in North America. J. Am. Mosq. Control Assoc. 28, 137–151.

Brault, A.C., 2009. Changing patterns of West Nile virus transmission: altered vector competence and host susceptibility. Vet. Res. 40, 43.

Britton, W.E., 1914. A remarkable outbreak of *Culex pipiens* Linn. J. Econ. Entomol. 7, 257–260.

Brown, H., Duik-Wasser, M., Andreadis, T., Fish, D., 2008a. Remotely-sensed vegetation indices identify mosquito clusters of West Nile virus vectors in an urban landscape in the northeastern United States. Vector Borne Zoonotic Dis. 8, 197–206.

Brown, H.E., Childs, J.E., Diuk-Wasser, M.A., Fish, D., 2008b. Ecological factors associated with West Nile virus transmission, northeastern United States. Emerg. Infect. Dis. 14, 1539–1545.

Brown, H.E., Paladini, M., Cook, R.A., Kline, D., Barnard, D., Fish, D., 2008c. Effectiveness of mosquito traps in measuring species abundance and composition. J. Med. Entomol. 45, 517–521.

Brownstein, J.S., Rosen, H., Purdy, D., Miller, J.R., Merlino, M., Mostashari, F., Fish, D., 2002. Spatial assessment of West Nile virus: rapid risk assessment of an introduced vectorborne zoonosis. Vector Borne Zoonotic Dis. 2, 157–164.

Brunsdon, C., Comber, L., 2015. An Introduction to R for Spatial Analysis and Mapping. Sage Publications LTD, London.

Busetto, L., Ranghetti, L., 2016. MODIStsp: an R package for automatic preprocessing of MODIS Land Products time series. Comput. Geosci. 97, 40–48.

Calhoun, L.M., Avery, M., Jones, L., Gunarto, K., King, R., Roberts, J., Burkot, T.R., 2007. Combined sewage overflows (CSO) are major urban breeding sites for *Culex quinquefasciatus* in Atlanta, Georgia. Am. J. Trop. Med. Hyg. 77, 478–484.

Cazelles, B., Chavez, M., De Magny, G.C., Guégan, J.-F., Hales, S., 2007. Time-dependent spectral analysis of epidemiological time-series with wavelets. J. R. Soc. Interface 4, 625–636.

CDC, 2016. Final Annual Maps & Data for 1999–2016. https://www.cdc.gov/westnile/statsmaps/finalmapsdata/index.html, Accessed date: 20 September 2018 (2016).

Chase, J.M., Knight, T.M., 2003. Drought-induced mosquito outbreaks in wetlands. Ecol. Lett. 6, 1017–1024.

Chaves, L.F., 2016. Globally invasive, withdrawing at home: *Aedes albopictus* and *Aedes japonicus* facing the rise of *Aedes flavopictus*. Int. J. Biometeorol. 60, 1727–1738.

Chaves, L.F., 2017. Climate Change and the Biology of Insect Vectors of Human Pathogens. John Wiley & Sons, Ltd.

Chaves, L.F., Kitron, U.D., 2011. Weather variability impacts on oviposition dynamics of the southern house mosquito at intermediate time scales. Bull. Entomol. Res. 101, 633–641.

Chaves, L.F., Koenraadt, C.J., 2010. Climate change and highland malaria: fresh air for a hot debate. Q. Rev. Biol. 85, 27–55.

Chaves, L.F., Pascual, M., 2006. Climate cycles and forecasts of cutaneous leishmaniasis, a nonstationary vector-borne disease. PLoS Med. 3, e295.

Chaves, L.F., Pascual, M., 2007. Comparing models for early warning systems of neglected tropical diseases. PLoS Negl. Trop. Dis. 1, e33.

Chaves, L.F., Keogh, C.L., Vazquez-Prokopec, G.M., Kitron, U.D., 2009. Combined sewage overflow enhances oviposition of Culex quinquefasciatus (Diptera: Culicidae) in urban areas. J. Med. Entomol. 46, 220–226.

Chaves, L.F., Hamer, G.L., Walker, E.D., Brown, W.M., Ruiz, M.O., Kitron, U.D., 2011a. Climatic variability and landscape heterogeneity impact urban mosquito diversity and vector abundance and infection. Ecosphere 2, 1–21.

Chaves, L.F., Keogh, C.L., Nguyen, A.M., Decker, G.M., Vazquez-Prokopec, G.M., Kitron, U.D., 2011b. Combined sewage overflow accelerates immature development and increases body size in the urban mosquito *Culex quinquefasciatus*. J. Appl. Entomol. 135, 611–620.

Chaves, L.F., Morrison, A.C., Kitron, U.D., Scott, T.W., 2012. Nonlinear impacts of climatic variability on the density-dependent regulation of an insect vector of disease. Glob. Chang. Biol. 18, 457–468.

Chaves, L.F., Higa, Y., Lee, S.H., Jeong, J.Y., Heo, S.T., Kim, M., Minakawa, N., Lee, K.H., 2013. Environmental forcing shapes regional house mosquito synchrony in a warming temperate island. Environ. Entomol. 42, 605–613.

Chaves, L.F., Calzada, J.E., Valderama, A., Saldaña, A., 2014. Cutaneous leishmaniasis and sand fly fluctuations are associated with El Niño in Panamá. PLoS Negl. Trop. Dis. 8, e3210.

Chaves, L.F., Jian, J.-Y., Moji, K., 2018. Overwintering in the bamboo mosquito *Tripteroides bambusa* (Diptera: Culicidae) during a warm, but unpredictably changing, winter. Environ. Entomol. 47, 148–158.

Chuang, T.-W., Hildreth, M.B., Vanroekel, D.L., Wimberly, M.C., 2011. Weather and land cover influences on mosquito populations in Sioux Falls, South Dakota. J. Med. Entomol. 48, 669–679.

Chuang, T.W., Hockett, C.W., Kightlinger, L., Wimberly, M.C., 2012. Landscape-level spatial patterns of West Nile virus risk in the northern Great Plains. Am. J. Trop. Med. Hyg. 86, 724–731.

Chuang, T.W., Chaves, L.F., Chen, P.J., 2017. Effects of local and regional climatic fluctuations on dengue outbreaks in southern Taiwan. PLoS One 12, e0178698.

Chung, W.M., Buseman, C.M., Joyner, S.N., Hughes, S.M., Fomby, T.B., Luby, J.P., Haley, R.W., 2013. The 2012 West Nile encephalitis epidemic in Dallas, Texas. JAMA 310, 297–307.

Ciota, A.T., Matacchiero, A.C., Kilpatrick, A.M., Kramer, L.D., 2014. The effect of temperature on life history traits of *Culex* mosquitoes. J. Med. Entomol. 51, 55–62.

Clements, A., 1992. The biology of mosquitoes. Development, Nutrition and Reproduction. vol I. Chapman Hall, Florida.

Connor, S., Thomson, M., Molyneux, D., 1999. Forecasting and prevention of epidemic malaria: new perspectives on an old problem. Parassitologia 41, 439–448.

Craig, M.H., Snow, R., le Sueur, D., 1999. A climate-based distribution model of malaria transmission in sub-Saharan Africa. Parasitol. Today 15, 105–111.

Curtis, A., Ye, X., Heob, E., Targhetta, J., Salvato, V., Reyna, M., Bueno, R., Holmes, L., 2014. A comparison of three approaches to identify West Nile virus mosquito space-time hotspots in the Houston Vicinity for the period 2002–2011. Appl. Geogr. 51, 58–64.

Darsie Jr., R.F., Ward, R.A., 2005. Identification and Geographical Distribution of the Mosquitoes of North America, North of Mexico. Second ed. University of Florida Press, Gainesville, FL.

Dawson, J.R., Stone, W.B., Ebel, G.D., Young, D.S., Galinski, D.S., Pensabene, J.P., Franke, M.A., Eidson, M., Kramer, L.D., 2007. Crow deaths caused by West Nile virus during winter. Emerg. Infect. Dis. 13, 1912.

Degaetano, A.T., 2005. Meteorological effects on adult mosquito (*Culex*) populations in metropolitan New Jersey. Int. J. Biometeorol. 49, 345–353.

Degroote, J.P., Sugumaran, R., Ecker, M., 2014. Landscape, demographic and climatic associations with human West Nile virus occurrence regionally in 2012 in the United States of America. Geospat. Health 9, 153–168.

Denlinger, D.L., Armbruster, P.A., 2014. Mosquito diapause. Annu. Rev. Entomol. 59, 73–93.

Dennett, J., Debboun, M., 2017. Case study: surveillance and control operations in Harris County, Texas. Pest Control Technology.

Dennett, J.A., Bala, A., Wuithiranyagool, T., Randle, Y., Sargent, C.B., Guzman, H., Siirin, M., Hassan, H.K., Reyna-Nava, M., Unnasch, T.R., Tesh, R.B., Parsons, R.E., Bueno, R., 2007a. Associations between two mosquito populations and West Nile virus in Harris County, Texas, 2003–061. J. Am. Mosq. Control Assoc. 23, 264–275.

Dennett, J.A., Wuithiranyagool, T., Reyna-Nava, M., Bala, A., Tesh, R.B., Parsons, R.E., Bueno, R., 2007b. Description and use of the Harris County gravid trap for West Nile virus surveillance 2003–061. J. Am. Mosq. Control Assoc. 23, 359–362.

Diaz-Badillo, A., Bolling, B.G., Perez-Ramirez, G., Moore, C.G., Martinez-Munoz, J.P., Padilla-Viveros, A.A., Camacho-Nuez, M., Diaz-Perez, A., Beaty, B.J., de Lourdes Munoz, M., 2011. The distribution of potential West Nile virus vectors, Culex pipiens pipiens and Culex pipiens quinquefasciatus (Diptera: Culicidae), in Mexico City. Parasit. Vectors 4, 70.

Didan, K., 2015. In: DAAC, N.E.L. (Ed.), MYD13A3 MODIS/Aqua Vegetation Indices Monthly L3 Global 1km SIN Grid V006.

Diniz, D.F.A., de Albuquerque, C.M.R., Oliva, L.O., de Melo-Santos, M.A.V., Ayres, C.F.J., 2017. Diapause and quiescence: dormancy mechanisms that contribute to the geographical expansion of mosquitoes and their evolutionary success. Parasit. Vectors 10, 310.

Dohm, D.J., Turell, M.J., 2001. Effect of incubation at overwintering temperatures on the replication of West Nile virus in New York Culex pipiens (Diptera: Culicidae). J. Med. Entomol. 38, 462–464.

Dohm, D.J., O'Guinn, M.L., Turell, M.J., 2002. Effect of environmental temperature on the ability of Culex pipiens (Diptera: Culicidae) to transmit West Nile virus. J. Med. Entomol. 39, 221–225.

Eldridge, B.F., 1968. The effect of temperature and photoperiod on blood-feeding and ovarian development in mosquitoes of the Culex pipiens complex. Am. J. Trop. Med. Hyg. 17, 133–140.

Faraway, J.J., 2016. Linear Models With R. Chapman and Hall/CRC.

Farrington, C., 1992. Estimating prevalence by group testing using generalized linear models. Stat. Med. 11, 1591–1597.

Forchhammer, M.C., Post, E., Stenseth, N.C., 1998. Breeding phenology and climate…. Nature 391, 29.

Fredregill, C.L., Motl, G.C., Dennett, J.A., Flatt, K.L., Bueno Jr., R., 2011. Thermal fog efficacy tests against mosquitoes in storm drains in Harris County, Texas 2008–09. J. Am. Mosq. Control Assoc. 27, 61–68.

Gardner, A.M., Anderson, T.K., Hamer, G.L., Johnson, D.E., Varela, K.E., Walker, E.D., Ruiz, M.O., 2013. Terrestrial vegetation and aquatic chemistry influence larval mosquito abundance in catch basins, Chicago, USA. Parasit. Vectors 6, 9.

Goddard, L.B., Roth, A.E., Reisen, W.K., Scott, T.W., 2003. Vertical transmission of West Nile virus by three California Culex (Diptera: Culicidae) species. J. Med. Entomol. 40, 743–746.

Hamer, G.L., Kitron, U.D., Brawn, J.D., Loss, S.R., Ruiz, M.O., Goldberg, T.L., Walker, E.D., 2008a. Culex pipiens (Diptera: Culicidae): a bridge vector of West Nile virus to humans. J. Med. Entomol. 45, 125–128.

Hamer, G.L., Walker, E.D., Brawn, J.D., Loss, S.R., Ruiz, M.O., Goldberg, T.L., Schotthoefer, A.M., Brown, W.M., Wheeler, E., Kitron, U.D., 2008b. Rapid amplification of West Nile virus: the role of hatch-year birds. Vector Borne Zoonotic Dis. 8, 57–67.

Hamer, G.L., Kelly, P.H., Focks, D.A., Goldberg, T.L., Walker, E.D., 2011. Evaluation of a novel emergence trap to study Culex mosquitoes in urban catch basins. J. Am. Mosq. Control Assoc. 27, 142–147.

Hayes, J., 1975. Seasonal changes in population structure of Culex pipiens quinquefasciatus say (Diptera: Culicidae): study of an isolated population. J. Med. Entomol. 12, 167–178.

Hayes, J., Downs, T.D., 1980. Seasonal changes in an isolated population of Culex pipiens quinquefasciatus (Diptera: Culicidae): a time series analysis. J. Med. Entomol. 17, 63–69.

Hayes, J., Hsi, B.P., 1975. Interrelationships between selected meteorologic phenomena and immature stages of Culex pipiens quinquefasciatus Say: study of an isolated population. J. Med. Entomol. 12, 299–308.

Heft, D.E., Walton, W.E., 2008. Effects of the El Niño-Southern Oscillation (ENSO) cycle on mosquito populations in southern California. J. Vector Ecol. 33, 17–29.

Hinton, M.G., Reisen, W.K., Wheeler, S.S., Townsend, A.K., 2015. West Nile virus activity in a winter roost of American crows (Corvus brachyrhynchos): is bird-to-bird transmission important in persistence and amplification? J. Med. Entomol. 52, 683–692.

Hoshi, T., Higa, Y., Chaves, L.F., 2014. Uranotaenia novobscura ryukyuana (Diptera: Culicidae) population dynamics are denso-dependent and autonomous from weather fluctuations. Ann. Entomol. Soc. Am. 107, 136–142.

Huang, B., Thorne, P.W., Banzon, V.F., Boyer, T., Chepurin, G., Lawrimore, J.H., Menne, M.J., Smith, T.M., Vose, R.S., Zhang, H.-M., 2017. Extended reconstructed sea surface temperature, version 5 (ERSSTv5): upgrades, validations, and intercomparisons. J. Clim. 30, 8179–8205.

Hunt, G.J., Hacker, C.S., 1984. Computer-generated maps as an aid to mosquito control (Diptera: Culicidae). J. Med. Entomol. 21, 489–500.

Hurtado, L.A., Cáceres, L., Chaves, L.F., Calzada, J.E., 2014. When climate change couples social neglect: malaria dynamics in Panamá. Emerg. Microbes Infect. 3, e28.

Hurtado, L.A., Calzada, J.E., Rigg, C.A., Castillo, M., Chaves, L.F., 2018. Climatic fluctuations and malaria transmission dynamics, prior to elimination, in Guna Yala, República de Panamá. Malar. J. 17, 85.

Kilpatrick, A.M., Kramer, L.D., Campbell, S.R., Alleyne, E.O., Dobson, A.P., Daszak, P., 2005. West Nile virus risk assessment and the bridge vector paradigm. Emerg. Infect. Dis. 11, 425–429.

KNMI, 2018. KNMI Climate Explorer. https://climexp.knmi.nl/start.cgi, Accessed date: 1 February 2018 (2018).

Koenraadt, C.J.M., Harrington, L., 2008. Flushing effect of rain on container-inhabiting mosquitoes Aedes aegypti and Culex pipiens (Diptera: Culicidae). J. Med. Entomol. 45, 28–35.

Kuhn, M., Johnson, K., 2013. Applied Predictive Modeling. Springer.

Kuhn, K., Campbell-Lendrum, D., Haines, A., Cox, J., Corvalán, C., Anker, M., 2005. Using Climate to Predict Infectious Disease Epidemics. WHO, Geneva.

Lacour, G., Chanaud, L., L'Ambert, G., Hance, T., 2015. Seasonal synchronization of diapause phases in Aedes albopictus (Diptera: Culicidae). PLoS One 10, e0145311.

Landesman, W.J., Allan, B.F., Langerhans, R.B., Knight, T.M., Chase, J.M., 2007. Inter-annual associations between precipitation and human incidence of West Nile virus in the United States. Vector Borne Zoonotic Dis. 7, 337–343.

Levins, R., 1968. Evolution in Changing Environments: Some Theoretical Explorations. Princeton University Press.

Levins, R., Awerbuch, T., Brinkmann, U., Eckardt, I., Epstein, P., Makhoul, N., de Possas, C.A., Puccia, C., Spielman, A., Wilson, M.E., 1994. The emergence of new diseases. Am. Sci. 82, 52–60.

Lewontin, R., Levins, R., 2000. Schmalhausen's law. Capital. Nat. Social. 11, 103–108.

Li, Z., Kafatos, M., 2000. Interannual variability of vegetation in the United States and its relation to El Nino/Southern Oscillation. Remote Sens. Environ. 71, 239–247.

Lillibridge, K.M., Parsons, R., Randle, Y., da Rosa, A.P.T., Guzman, H., Siirin, M., Wuithiranyagool, T., Hailey, C., Higgs, S., Bala, A.A., 2004. The 2002 introduction of West Nile virus into Harris County, Texas, an area historically endemic for St. Louis encephalitis. Am. J. Trop. Med. Hyg. 70, 676–681.

Lowe, R., Bailey, T.C., Stephenson, D.B., Jupp, T.E., Graham, R.J., Barcellos, C., Carvalho, M.S., 2013. The development of an early warning system for climate-sensitive disease risk with a focus on dengue epidemics in Southeast Brazil. Stat. Med. 32, 864–883.

Manore, C.A., Davis, J., Christofferson, R.C., Wesson, D., Hyman, J.M., Mores, C.N., 2014. Towards an early warning system for forecasting human West Nile virus incidence. PLoS Curr. 6.

Molaei, G., Andreadis, T.G., Armstrong, P.M., Bueno Jr., R., Dennett, J.A., Real, S.V., Sargent, C., Bala, A., Randle, Y., Guzman, H., Travassos da Rosa, A., Wuithiranyagool, T., Tesh, R.B., 2007. Host feeding pattern of Culex quinquefasciatus (Diptera: Culicidae) and its role in transmission of West Nile virus in Harris County, Texas. Am. J. Trop. Med. Hyg. 77, 73–81.

Montecino-Latorre, D., Barker, C.M., 2018. Overwintering of West Nile virus in a bird community with a communal crow roost. Sci. Rep. 8, 6088.

Morris, C., DeFoliart, G., 1969. A comparison of mosquito catches with miniature light traps and CO2-baited traps. Mosq. News 29, 424–426.

Murray, K.O., Ruktanonchai, D., Hesalroad, D., Fonken, E., Nolan, M.S., 2013. West Nile virus, Texas, USA, 2012. Emerg. Infect. Dis. 19, 1836–1838.

NASA, 2018. LP DAAC. https://lpdaac.usgs.gov/, Accessed date: 1 February 2018 (2018).

Nelms, B.M., Macedo, P.A., Kothera, L., Savage, H.M., Reisen, W.K., 2013. Overwintering biology of Culex (Diptera: Culicidae) mosquitoes in the Sacramento Valley of California. J. Med. Entomol. 50, 773–790.

Ng, K.C., Chaves, L.F., Tsai, K.H., Chuang, T.W., 2018. Increased adult Aedes aegypti and Culex quinquefasciatus (Diptera: Culicidae) abundance in a dengue transmission hotspot, compared to a Coldspot, within Kaohsiung City, Taiwan. Insects 9.

Nguyen, A.T., Williams-Newkirk, A.J., Kitron, U.D., Chaves, L.F., 2012. Seasonal weather, nutrients, and conspecific presence impacts on the southern house mosquito oviposition dynamics in combined sewage overflows. J. Med. Entomol. 49, 1328–1338.

NOAA ESRL, 2018a. GHCN_CAMS gridded 2m temperature (land). https://www.esrl.noaa.gov/psd/data/gridded/data.ghcncams.html, Accessed date: 1 February 2018 (2018).

NOAA ESRL, 2018b. GPCP version 2.3 combined precipitation data set. https://www.esrl.noaa.gov/psd/data/gridded/data.gpcp.html, Accessed date: 1 February 2018 (2018).

NOAA National Weather Service, 2018. 2018. Climate Prediction Center. http://www.cpc.ncep.noaa.gov/, Accessed date: 1 February 2018.

Nolan, M.S., Zangeneh, A., Khuwaja, S.A., Martinez, D., Rossmann, S.N., Cardenas, V., Murray, K.O., 2012. Proximity of residence to bodies of water and risk for West Nile virus infection: a case-control study in Houston, Texas. J Biomed Biotechnol 2012, 159578.

Paz, S., Semenza, J.C., 2013. Environmental drivers of West Nile fever epidemiology in Europe and Western Asia—a review. Int. J. Environ. Res. Public Health 10, 3543–3562.

Pettorelli, N., Vik, J.O., Mysterud, A., Gaillard, J.-M., Tucker, C.J., Stenseth, N.C., 2005. Using the satellite-derived NDVI to assess ecological responses to environmental change. Trends Ecol. Evol. 20, 503–510.

Ponnusamy, L., Xu, N., Stav, G., Wesson, D.M., Schal, C., Apperson, C.S., 2008. Diversity of bacterial communities in container habitats of mosquitoes. Microb. Ecol. 56, 593–603.

Randle, Y.H., Freeman, C.B., Jackson, M., Reyna, M., Debboun, M., 2016. 2014: a record-breaking year for West Nile virus positive mosquito pools in Harris County and the city of Houston, Texas. US Army Med. Dep. J. 3-16, 1–8.

Randolph, S.E., Rogers, D.J., 2010. The arrival, establishment and spread of exotic diseases: patterns and predictions. Nat. Rev. Microbiol. 8, 361–371.

Reisen, W.K., 1995. Effect of temperature on Culex tarsalis (Diptera: Culicidae) from the Coachella and San Joaquin valleys of California. J. Med. Entomol. 32, 636–645.

Reisen, W.K., 2012. The contrasting bionomics of Culex mosquitoes in western North America. J. Am. Mosq. Control Assoc. 28, 82–91.

Reisen, W.K., Meyer, R.P., Milby, M.M., 1986. Overwintering studies on Culex tarsalis (Diptera: Culicidae) in Kern County, California: temporal changes in abundance and reproductive status with comparative observations on C. quinquefasciatus (Diptera: Culicidae). Ann. Entomol. Soc. Am. 79, 677–685.

Reisen, W.K., Fang, Y., Lothrop, H.D., Martinez, V.M., Wilson, J., O'Connor, P., Carney, R., Cahoon-Young, B., Shafii, M., Brault, A.C., 2006a. Overwintering of West Nile virus in Southern California. J. Med. Entomol. 43, 344–355.

Reisen, W.K., Fang, Y., Martinez, V.M., 2006b. Effects of temperature on the transmission of West Nile virus Culex tarsalis (Diptera: Culicidae). J. Med. Entomol. 43, 309–317.

Reisen, W.K., Cayan, D., Tyree, M., Barker, C.M., Eldridge, B., Dettinger, M., 2008. Impact of climate variation on mosquito abundance in California. J. Vector Ecol. 33, 89–98.

Reisen, W.K., Thiemann, T., Barker, C.M., Lu, H., Carroll, B., Fang, Y., Lothrop, H.D., 2010. Effects of warm winter temperature on the abundance and gonotrophic activity of Culex (Diptera: Culicidae) in California. J. Med. Entomol. 47, 230–237.

Rigg, C.A., Hurtado, L.A., Calzada, J.E., Chaves, L.F., 2019. Malaria infection rates in Anopheles albimanus (Diptera: Culicidae) at Ipetí-Guna, a village within a region targeted for malaria elimination in Panamá. Infect. Genet. Evol. 69, 216–223.

Rios, J., Hacker, C.S., Hailey, C.A., Parsons, R.E., 2006. Demographic and spatial analysis of West Nile virus and St. Louis encephalitis in Houston, Texas. J. Am. Mosq. Control Assoc. 22, 254–263.

Rogers, D.J., Randolph, S.E., 2003. Studying the global distribution of infectious diseases using GIS and RS. Nat. Rev. Microbiol. 1, 231–237.

Rueda, L., Patel, K., Axtell, R., Stinner, R., 1990. Temperature-dependent development and survival rates of Culex quinquefasciatus and Aedes aegypti (Diptera: Culicidae). J. Med. Entomol. 27, 892–898.

Ruiz, M.O., Tedesco, C., McTighe, T.J., Austin, C., Kitron, U., 2004. Environmental and social determinants of human risk during a West Nile virus outbreak in the greater Chicago area, 2002. Int. J. Health Geogr. 3, 1–11.

Ruiz, M.O., Chaves, L.F., Hamer, G.L., Sun, T., Brown, W.M., Walker, E.D., Haramis, L., Goldberg, T.L., Kitron, U.D., 2010. Local impact of temperature and precipitation on West Nile virus infection in Culex species mosquitoes in northeast Illinois, USA. Parasit. Vectors 3, 19.

Shaman, J., Day, J.F., 2005. Achieving operational hydrologic monitoring of mosquitoborne disease. Emerg. Infect. Dis. 11, 1343.

Shaman, J., Day, J.F., 2007. Reproductive phase locking of mosquito populations in response to rainfall frequency. PLoS ONE 2, e331.

Shaman, J., Stieglitz, M., Stark, C., Le Blancq, S., Cane, M., 2002. Using a dynamic hydrology model to predict mosquito abundances in flood and swamp water. Emerg. Infect. Dis. 8, 6–13.

Shand, L., Brown, W.M., Chaves, L.F., Goldberg, T.L., Hamer, G.L., Haramis, L., Kitron, U., Walker, E.D., Ruiz, M.O., 2016. Predicting West Nile virus infection risk from the synergistic effects of rainfall and temperature. J. Med. Entomol. 53, 935–944.

Shumway, R.H., Stoffer, D.S., 2011. Time Series Regression and Exploratory Data Analysis, Time Series Analysis and Its Applications. Springer, pp. 47–82.

Siirin, M., Sargent, C., Langer, R.C., Parsons, R., Vanlandingham, D.L., Higgs, S., Tesh, R.B., 2004. Comparative sensitivity of the VecTest antigen-capture assay, reverse transcriptase-PCR, and cell culture for detection of West Nile virus in dead birds. Vector Borne Zoonotic Dis. 4, 204–209.

Smith, C.G., 1987. Factors influencing the transmission of western equine encephalomyelitis virus between its vertebrate maintenance hosts and from them to humans. Am. J. Trop. Med. Hyg. 37, 33S–39S.

Soverow, J.E., Wellenius, G.A., Fisman, D.N., Mittleman, M.A., 2009. Infectious disease in a warming world: how weather influenced West Nile virus in the United States (2001–2005). Environ. Health Perspect. 117, 1049–1052.

Speybroeck, N., Williams, C.J., Lafia, K.B., Devleesschauwer, B., Berkvens, D., 2012. Estimating the prevalence of infections in vector populations using pools of samples. Med. Vet. Entomol. 26, 361–371.

Strickman, D., 1983. Preliminary report of seasonal oviposition by Culex quinquefasciatus in San Antonio, Texas. Mosq. News 43, 226–230.

Strickman, D., 1988. Rate of oviposition by Culex quinquefasciatus in San Antonio, Texas, during three years. J. Am. Mosq. Control Assoc. 4, 339–344.

Strickman, D., Lang, J.T., 1986. Activity of Culex quinquefasciatus in an underground storm drain in San Antonio, Texas. J. Am. Mosq. Control Assoc. 2, 379–381.

Takeda, T., Whitehouse, C.A., Brewer, M., Gettman, A.D., Mather, T.N., 2003. Arbovirus surveillance in Rhode Island: assessing potential ecologic and climatic correlates. J. Am. Mosq. Control Assoc. 19, 179–189.

Thomson, M., Connor, S., 2000. Environmental information systems for the control of arthropod vectors of disease. Med. Vet. Entomol. 14, 227–244.

Thomson, M.C., Doblas-Reyes, F.J., Mason, S.J., Hagedorn, R., Connor, S.J., Phindela, T., Morse, A.P., Palmer, T.N., 2006. Malaria early warnings based on seasonal climate forecasts from multi-model ensembles. Nature 439, 576–579.

Turell, M.J., Dohm, D.J., Sardelis, M.R., O'guinn, M.L., Andreadis, T.G., Blow, J.A., 2005. An update on the potential of North American mosquitoes (Diptera: Culicidae) to transmit West Nile virus. J. Med. Entomol. 42, 57–62.

United States Census Bureau, 2018. QuickFacts. https://www.census.gov/quickfacts/fact/table/US/PST045217, Accessed date: 1 February 2018 (2016).

Venables, W.N., Ripley, B.D., 2002. Modern Applied Statistics With S. Springer, New York.

Vezzani, D., 2007. Review: artificial container-breeding mosquitoes and cemeteries: a perfect match. Tropical Med. Int. Health 12, 299–313.

Vinogradova, E.B., 2007. Diapause in aquatic insects, with emphasis on mosquitoes. Diapause in Aquatic Invertebrates Theory and Human Use. Springer, pp. 83–113.

Walther, G.-R., Post, E., Convey, P., Menzel, A., Parmesan, C., Beebee, T.J., Fromentin, J.-M., Hoegh-Guldberg, O., Bairlein, F., 2002. Ecological responses to recent climate change. Nature 416, 389.

Ward, M.P., Ramsay, B.H., Gallo, K., 2005. Rural cases of equine West Nile virus encephalomyelitis and the normalized difference vegetation index. Vector Borne Zoonotic Dis. 5, 181–188.

Weaver, S.C., Reisen, W.K., 2010. Present and future arboviral threats. Antivir. Res. 85, 328–345.

White, S.L., Ward, M.P., Budke, C.M., Cyr, T., Bueno Jr., R., 2009. A comparison of gravid and under-house CO2-baited CDC light traps for mosquito species of public health importance in Houston, Texas. J. Med. Entomol. 46, 1494–1497.

Wimberly, M.C., Lamsal, A., Giacomo, P., Chuang, T.W., 2014. Regional variation of climatic influences on West Nile virus outbreaks in the United States. Am. J. Trop. Med. Hyg. 91, 677–684.

Winters, A.M., Eisen, R.J., Delorey, M.J., Fischer, M., Nasci, R.S., Zielinski-Gutierrez, E., Moore, C.G., Pape, W.J., Eisen, L., 2010. Spatial risk assessments based on vector-borne disease epidemiologic data: importance of scale for West Nile virus disease in Colorado. Am. J. Trop. Med. Hyg. 82, 945–953.